2-2009

Partially Adaptive STAP Algorithm Approaches to Functional MRI

L. Huang

Elizabeth A. Thompson
Indiana University - Purdue University Fort Wayne, thompsoe@ipfw.edu

V. Schmithorst

S. K. Holland

T. M. Talavage

Partially adaptive STAP algorithm approaches to functional MRI.

ARTICLE *in* IEEE TRANSACTIONS ON BIO-MEDICAL ENGINEERING · MARCH 2009

Impact Factor: 2.23 · DOI: 10.1109/TBME.2008.2006017 · Source: PubMed

5 AUTHORS, INCLUDING:

Scott K Holland
Cincinnati Children's Hospital Medical Center
239 PUBLICATIONS **6,413** CITATIONS

Published in final edited form as:
IEEE Trans Biomed Eng. 2009 February ; 56(2): 518–521. doi:10.1109/TBME.2008.2006017.

Partially Adaptive STAP Algorithm Approaches to functional MRI

Lejian Huang,
School of Electrical and Computer Engineering, Purdue University, West Lafayette, IN 47907

Elizabeth A. Thompson [Member, IEEE],
Department of Engineering, Purdue University, Ft. Wayne, IN 46805 (thompson@engr.ipfw.edu).

Vincent Schmithorst,
Imaging Research Center, Children's Hospital Medical Center, Cincinnati, OH 45229

Scott K. Holland [Member, IEEE], and
Imaging Research Center, Children's Hospital Medical Center, Cincinnati, OH 45229

Thomas M. Talavage [Member, IEEE]
School of Electrical and Computer Engineering, Purdue University, West Lafayette, IN 47907

Abstract

In this work, the architectures of three partially adaptive STAP algorithms are introduced, one of which is explored in detail, that reduce dimensionality and improve tractability over fully adaptive STAP when used in construction of brain activation maps in fMRI. Computer simulations incorporating actual MRI noise and human data analysis indicate that element space partially adaptive STAP can attain close to the performance of fully adaptive STAP while significantly decreasing processing time and maximum memory requirements, and thus demonstrates potential in fMRI analysis.

Keywords

Element-space partially adaptively STAP; fMRI; image processing; space-time adaptive processing

I. Introduction

SPACE-TIME adaptive processing (STAP), originally developed for radar signal processing [1], has recently been shown to exhibit potential for detecting cortical activations in functional magnetic resonance imaging (fMRI) [2]-[5]. Unlike the methods in [6][7], it is not a subspace approach. Rather, it is a Fourier-based joint beamformer-frequency filter. Previous research in applying STAP to fMRI has focused on a fully adaptive version of the algorithm, which is computationally intensive because it applies a separate adaptive weight to every data point in the 2D or 3D data set. Here we introduce a partially adaptive STAP scheme to reduce dimensionality of the algorithm and make it more tractable.

Partially adaptive STAP was first introduced by Brennan and Reed in the form of element/beamspace algorithms [1][8]. For the partially adaptive implementation, a large set of input signals is first transformed into a smaller number of signals prior to applying STAP. The goal is to reduce processing time relative to fully adaptive STAP while maintaining comparable ability to detect true positives without introducing false positives. The method of element space

(lejian@purdue.edu; tmt@purdue.edu). (Vince.Schmithorst@cchmc.org; Scott.Holland@cchmc.org)..

is described in this paper, adapted for application to fMRI, and demonstrated to perform comparably with standard fMRI analysis techniques.

II. Theory

A. Generic Partially Adaptive STAP

The architecture of partially adaptive STAP consists of three parts: partially-selective processor, partially-adaptive processor and post-processor. The partially-selective processor is a non-adaptive preprocessor comprising two components—a temporal filter $\mathbf{J}_p$ and a spatial filter $\mathbf{G}_S$, which act as selection matrices to reduce the amount of data to be adaptively processed. The partially-adaptive processor computes a weight matrix for each of the resulting reduced dimension data sets in the same manner that fully adaptive STAP computes a weight matrix for a full dimension data set. The post-processor then combines these individual weights for the data subsets of the partially-adaptive processor into a single full dimensional composite weight matrix. From this point, processing is identical to that of fully adaptive STAP in which the weights are applied to the full dimensional input data set to obtain the STAP filter outputs.

Combinations of temporal and/or spatial filtering using $\mathbf{J}_p$ and $\mathbf{G}_s$ in the partially-selective processor unit compose the different types of partially adaptive STAP [8]. Element space partially adaptive STAP retains the spatial dimensionality of fully adaptive STAP but reduces the number of temporal degrees of freedom prior to adaptation. Beamspace partially adaptive STAP reduces only the spatial dimensionality prior to adaptation in the partially-adaptive processor. Element-beamspace partially adaptive STAP reduces both temporal and spatial dimensionality. For economy, only the element-space method is discussed in detail here because it is the most promising of the three partially adaptive schemes investigated.

B. Temporal and Spatial Steering Matrices

STAP is a two-dimensional filter which simultaneously determines spatial location and frequency of cortical activations. STAP requires both a spatial steering matrix, which controls the ability of the algorithm to correctly locate the fMRI activation in space, and also a temporal steering matrix, which dictates its ability to properly identify the frequency/frequencies of fMRI activation. In [2], Thompson, et al. defined a spatial steering matrix, $\mathbf{A}(x, y)$, to be applied to k-space, representing the activation patterns and spatial locations of all possible activations. In [9], the model was simplified for application to image space fMRI data, reducing the Hermitian transpose in many of the STAP equations to a simple transpose, given that data in image space are real-valued (magnitude images) rather than complex. However, in the discussion below, the more general formula for complex valued data is provided with the understanding that real data is a subset of this general case.

The temporal steering matrix for activation frequency ω, similar to that in [2], is

$$\mathbf{B}(\omega) = \begin{bmatrix} 1 & e^{j2\pi\omega_1} & e^{j2\pi\omega_1\cdot 2} & \dots e^{j2\pi\omega_1\cdot(N-1)} \\ \dots & \dots & \dots & \dots \\ 1 & e^{j2\pi\omega_k} & e^{j2\pi\omega_k\cdot 2} & \dots e^{j2\pi\omega_k\cdot(N-1)} \end{bmatrix}^T, \quad (1)$$

where N and k represent the number of time points and the number of known frequencies of activation, respectively, associated with periodic task or stimulus presentations. The reduction of the temporal steering matrix to include only the frequencies in which we are interested represents a revision from that presented in our original work of [2], [3], and [5].

As in [2], the spatiotemporal steering matrix is defined as

$$\mathbf{V}=\mathbf{B}(\omega)\otimes\mathbf{A}(x,y) \tag{2}$$

and represents all combinations in space and frequency where activations may occur. The symbol ⊗ denotes Kronecker product.

C. The Scheme of Element Space Partially Adaptive STAP

Element space partially adaptive STAP retains the spatial dimensionality of fully adaptive STAP but reduces the number of temporal degrees of freedom prior to adaptation. It does so by combining the time course data of the 3D data sets into several subsets prior to computing reduced weights. Thus, a subset is defined comprising K_t successive frames from a full $M_x \times M_y \times N$ data set. As a result, the full data set is transformed into $N'=N/K_t$ non-overlapping subsets, each consisting of the full $M_x \times M_y$ spatial dimensionality but reduced to K_t frames. The reduction of the data set is accomplished via

$$\vec{\chi}_p=\left(\mathbf{J}_p\otimes\mathbf{I}_M\right)^H\vec{\chi}_{\mathrm{u}}, \tag{3}$$

where p represents the pth subset (p = 0, 1,... N'–1), H denotes hermitian transpose, $\vec{\chi}_{\mathrm{u}}$ is the original full dimensional column-wise reshaped resting state (baseline) data set as defined in [2], $\mathbf{I}_M$ is an identity matrix of size $M = M_x \times M_y$, and $\mathbf{J}_p$ is a selection matrix defined as

$$\mathbf{J}_p=\left[0_{pK_t\times K_t};\mathbf{I}_{K_t};0_{(N-pK_t-K_t)\times K_t}\right] \tag{4}$$

which chooses a particular subset of frames. The notation $0_{pK_t\times K_t}$ and $0_{(N-pK_t-K_t)\times K_t}$ refer to $pK_t \times K_t$ and $(N - pK_t - K_t) \times K_t$ matrix of zeros, respectively. For each subset p, a reduced weight matrix, $\mathbf{W}_p$ is calculated as

$$\mathbf{W}_p=\mathbf{R}_{\mathbf{u}p}^{-1}\mathbf{V}_p, \tag{5}$$

where

$$\mathbf{R}_{\mathbf{u}p}=E\left\{\vec{\chi}_p\vec{\chi}_p^H\right\} \tag{6}$$

and

$$\mathbf{V}_p=\left(\mathbf{J}_p\otimes\mathbf{I}_M\right)^H\mathbf{V} \tag{7}$$

where $\mathbf{R}_{\mathbf{u}p}$ is the reduced noise correlation matrix with $E\{\ \}$ denoting the expected value, and $\mathbf{V}_p$ is the reduced spatiotemporal steering matrix. The individual weights (p = 0, 1,... *N'-1)* obtained from (5) form the output of the partially adaptive processor. Note that a recursive algorithm solving (5) is introduced in [3]. Then we combine these reduced weights $\mathbf{W}_0$, $\mathbf{W}_1 ... \mathbf{W}_{N'-1}$ within the post-processor unit to form a single weight matrix $\mathbf{W}$ via

$$\mathbf{W}=\sum_{p=0}^{N-1}\left(\mathbf{J}_p\otimes\mathbf{I}_M\right)\mathbf{W}_p\left(diag\left(\mathbf{W}_p{}^H\mathbf{V}_p\right)\right) \tag{8}$$

where *diag* returns a diagonal matrix. Equation (8) has been adapted from Seliktar et al. [10] to accommodate a spatiotemporal steering matrix and a corresponding weight matrix rather than vectors. This weight matrix **W** is subsequently used to obtain the filter output,

$$\vec{z}=\mathbf{W}^H\vec{\chi}. \tag{9}$$

Here, $\vec{\chi}$ is the original column-wise reshaped activated data signal of full dimensionality as defined in [2]. This filter output consists of one frame for each of the stimulus frequencies present rather than output frames for all possible frequencies as represented by the DFT. Note that since $\vec{z}$ is complex, it can potentially provide phase information about the signal, in addition to the frequency and location information inherent to STAP.

III. Methods

A. Simulations

Validation of the proposed algorithm was effected using synthetic activation data superimposed on human baseline data. For purposes of comparison to the previously incorporated fully adaptive STAP techniques presented in [2][3], subsets of the same 64× 64× 1490 human data set were used here. For the simulations, reduced data sets of size 10 × 10× 60 were extracted so as to maintain the spatial and temporal continuity of the original data set. Two sets of *in vivo* images were used for the simulation. A time series of fMRI data, χ_u, was first acquired from a subject in the resting state, with no stimulation, in order to establish the baseline signal characteristics of the echo planar image data and to estimate the reduced noise correlation matrix, $\mathbf{R}_{up}$. In the same subject we also obtained a second resting state fMRI data set and then superimposed simulated activation in 10 voxels from a subset of 100 voxels in the image time series by adding a simulated activation signal (square wave) with amplitude of 4% relative to the mean intensity value of the time course data.

The first set of simulations was performed to establish suitable values for the parameter K_t of (4). Simulations were conducted on seven distinct subsets. The number of true positives (TP) and false positives (FP) were recorded as a function of threshold, and averaged over each of the seven data set simulations, providing a measure of algorithm performance. In addition, measures of CPU time and maximum memory requirements as a function of the parameter K_t were assessed.

Having identified a preferred value for the parameter K_t, another set of simulations was performed to compare the existing and widely-used fMRI analysis method of cross-correlation [11] to fully and partially adaptive STAP. Each of the three algorithms was tested using the same seven data subsets noted above, and results were averaged to obtain composite receiver-operator-characteristic (ROC) curves [12]. Furthermore, to illustrate the consistency of STAP results at lower signal intensity, additional simulations were run using a response amplitude of 2% relative to the mean intensity value of the time course data.

B. Human Data Analysis

To demonstrate that the proposed algorithm can be applied to actual human activation data, human data were collected from an fMRI experiment in which two blocked paradigms were

conducted in an overlapping manner: (1) a finger-tapping activity with period 60 s, and (2) visual stimulation (flickering checkerboard) with period 40 s. Echo-planar images were acquired using the following parameters: TR/TE = 3000/38 ms; FOV = 25.6 cm × 25.6 cm; BW = 125 kHz; 24 axial slices; 5 mm slice thickness; 120 time points; acquisition matrix = 64 × 64. Given that it is impossible to know the true activation region in a human experiment, it is necessary to choose a traditional analysis scheme as a gold-standard for subsequent comparison. For this work, the STAP algorithms were compared with the simple and widely-used cross-correlation and general linear model (GLM) approaches [13].

IV. Results And Discussion

A. Element Space Partially Adaptive STAP

Table I displays the average result for each tested K_t as a function of threshold. Instances in which all 10 activated voxels were successfully identified with no false positives are highlighted in bold. From Table I, we observe that for these simulations, element space partially adaptive STAP attains its highest degree of detection accuracy at thresholds between 0.4 and 0.6, but that performance is relatively independent of K_t. Therefore, factors such as CPU time and memory usage are likely more important in selection of a suitable value of K_t than is degree of detection accuracy.

Thus, given a desired detection accuracy, K_t may be selected to achieve a balance between processing time and memory requirements. Fig. 1 displays the CPU time and memory requirements as a function of K_t. It may be seen that both requirements increase with increasing K_t, with memory increasing as the square of K_t for fixed values of M_x and M_y. Therefore, for many data processing applications (particularly fMRI) in which data are large and memory requirements are generally of greater concern than processing time, $K_t = 1$ is a better option than $K_t = 2$. For small data sets, such as are used in the synthetic analysis, $K_t = 2$ would be optimal, but given an interest in the more general case, this value was not selected.

B. Synthetic Data Comparison

Fig. 2 depicts the ROC curves for the three tested algorithms as computed based on simulations with each of 4% and 2% activation. The ROC curves indicate that both element space and fully adaptive STAP exhibited better detection accuracy than cross-correlation in the simulations. Further, the performance of element space partially adaptive STAP was nearly equal to that of fully adaptive STAP.

C. Human Data Comparison

Results from single slices within (a) the motor and somatosensory cortices and (b) the primary visual cortex in a single subject are presented in Fig. 3. Note that the activation maps obtained for both forms of STAP are, for both the motor and visual tasks, consistent with those obtained using cross-correlation and GLM analysis. The selected slices in sensory motor cortex and visual cortex were chosen as examples from the full 24-slice data set to demonstrate the sensitivity of the partially adaptive STAP algorithm for detection of brain activation in expected locations. As seen in Fig. 3, element space partially adaptive STAP produced results nearly identical to those of fully adaptive STAP while the latter required triple the computation time. Therefore, element space partially adaptive STAP produces appropriate results and can significantly reduce the processing time and memory requirement, making it practical to use this spatio-temporal analysis procedure on human data.

V. Conclusions

We introduced a partially adaptive version to reduce dimensionality and improve tractability over that of fully adaptive STAP. The use of known activations, in the form of superimposed simulated activations enabled an objective and accurate comparison to the widely accepted method of cross-correlation.

Element space partially adaptive STAP exhibits potential in detecting cortical activations in fMRI and in reducing processing time and/or memory requirements of fully adaptive STAP. Within a wide range of parameters that specify the size of the reduced dimension data sets, element space partially adaptive STAP can exhibit better accuracy in detecting true activations than that of cross-correlation while greatly reducing running time and memory requirements of fully adaptive STAP. Human data analysis showed that the functional map of element space partially adaptive STAP was almost identical to that of fully adaptive STAP, and both were consistent with cross-correlation and the GLM approach.

Acknowledgments

This work was supported by NIH grant 1R21MH68267-01A1 and NIH grant 1R01EB003990.

References

1. Brennan L, Reed L. Theory of adaptive radar. IEEE Trans. Aero. and Elect. Sys 1973;9(2):237–252.
2. Thompson E, Holland S, Schmithorst V. A STAP algorithm approach to fMRI: a simulation study. J.Magn.Reson.Imaging 2004;20:715–722. [PubMed: 15390141]
3. Thompson E, Holland S, Schmithorst V. Detecting cortical activations from fMRI data using a recursive STAP algorithm. In Proc. IEEE ISBI'04 2004:976–979.
4. Thompson E. A parallel approach to STAP implementation for fMRI data. J. Magn.Reson. Imaging 2006;23:216–221. [PubMed: 16416435]
5. Huang L, Thompson E, Talavage TM. A partially adaptive STAP algorithm approach to fMRI. Proc. of the 13th ISMRM 2005:1578.
6. Sekihara K, Koizumi H. Detecting cortical activities from fMRI time-course data using the MUSIC algorithm with forward and backward covariance averaging. Magn. Reson. Med 1996;35:807–813. [PubMed: 8744006]
7. Chen H, Yao D, Chen W, Chen L. Delay correlation subspace decomposition algorithm and its Application in fMRI. IEEE Trans. Medical imaging 2005;24:1647–1650.
8. Ward, J. Space-time adaptive processing for airborne radar. Lincoln Laboratory, MIT; Lexington, MA: Dec. 13. 1994 Technical report 1015
9. Huang L, Thompson E, Comer M, Talavage TM, Holland S, Schmithorst V. An improved space-time adaptive processing model: a spatiotemporal approach for fMRI. Proc. IEEE 32nd NEBC 2007:49–50.
10. Seliktar Y, Williams DB, McClellan JH. Evaluation of partially adaptive STAP algorithms on the mountain top data set. Proc IEEE ICASSP 1996:1169–1172.
11. Bandettini PA, Jesmanowicz A, Wong EC, Hyde JS. Processing strategies for time-course data sets in functional MRI of the human brain. Magn.Reson.Med 1993;30:161–173. [PubMed: 8366797]
12. Constable R, Skudlarski P, Gore J. An ROC approach for evaluating functional brain MR imaging and postprocessing protocols. Magn.Reson.Med 1995;34:57–64. [PubMed: 7674899]
13. Friston KJ, Holmes AP, Worsley KJ, Poline JP, Frith CD, Frackowiak RSJ. Statistical parametric maps in functional imaging: a general linear approach. Human Brain Mapping 1995;2:189–210.

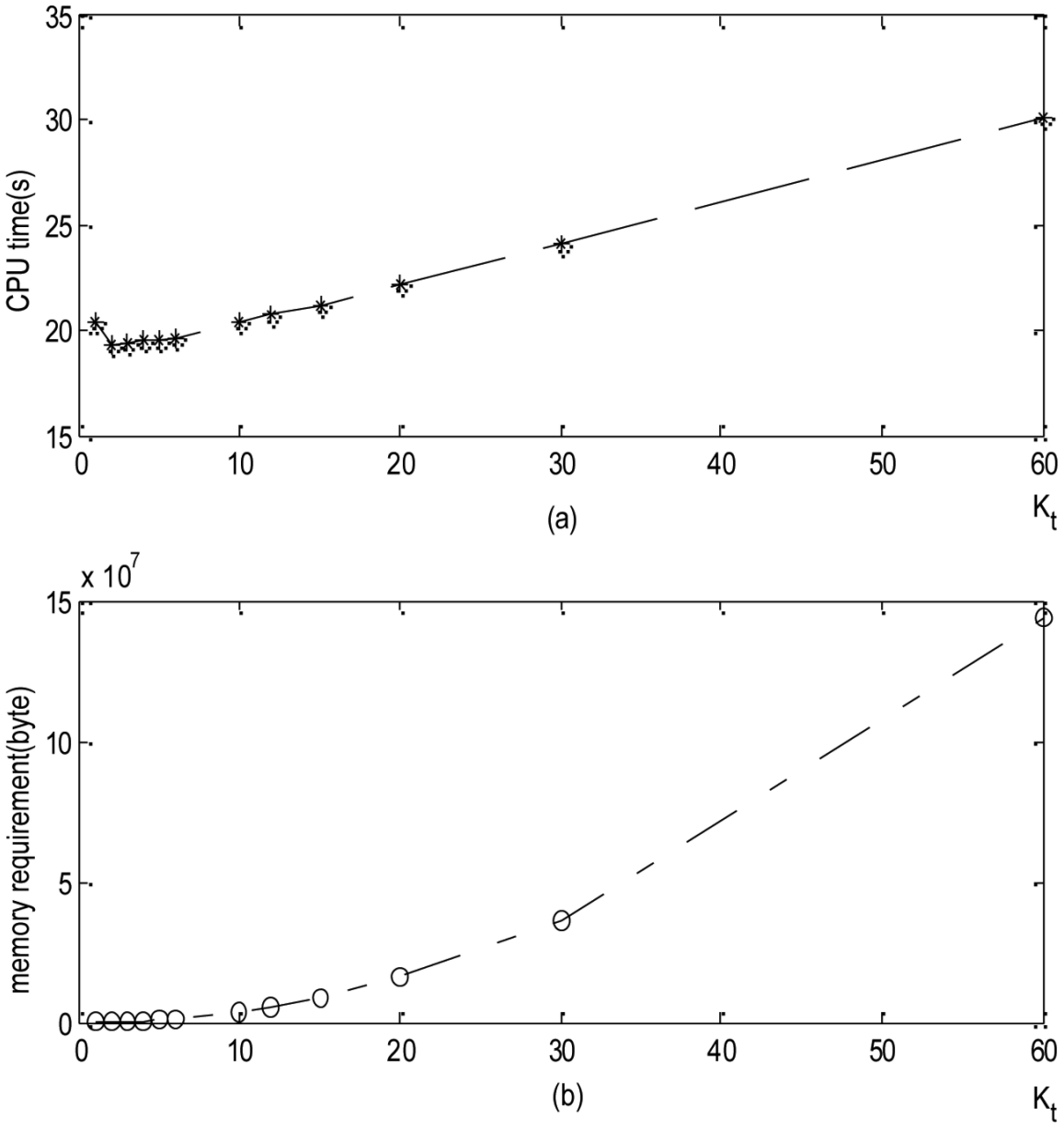

Fig. 1.

Processing performance of element-space partially adaptive STAP on a 10 × 10 × 60 dataset, as a function of K_t, with no reduction in spatial dimensionality (K_t = 60 corresponds to fully STAP). Graphs depict (top) CPU time, in seconds, and (bottom) memory requirements, in bytes.

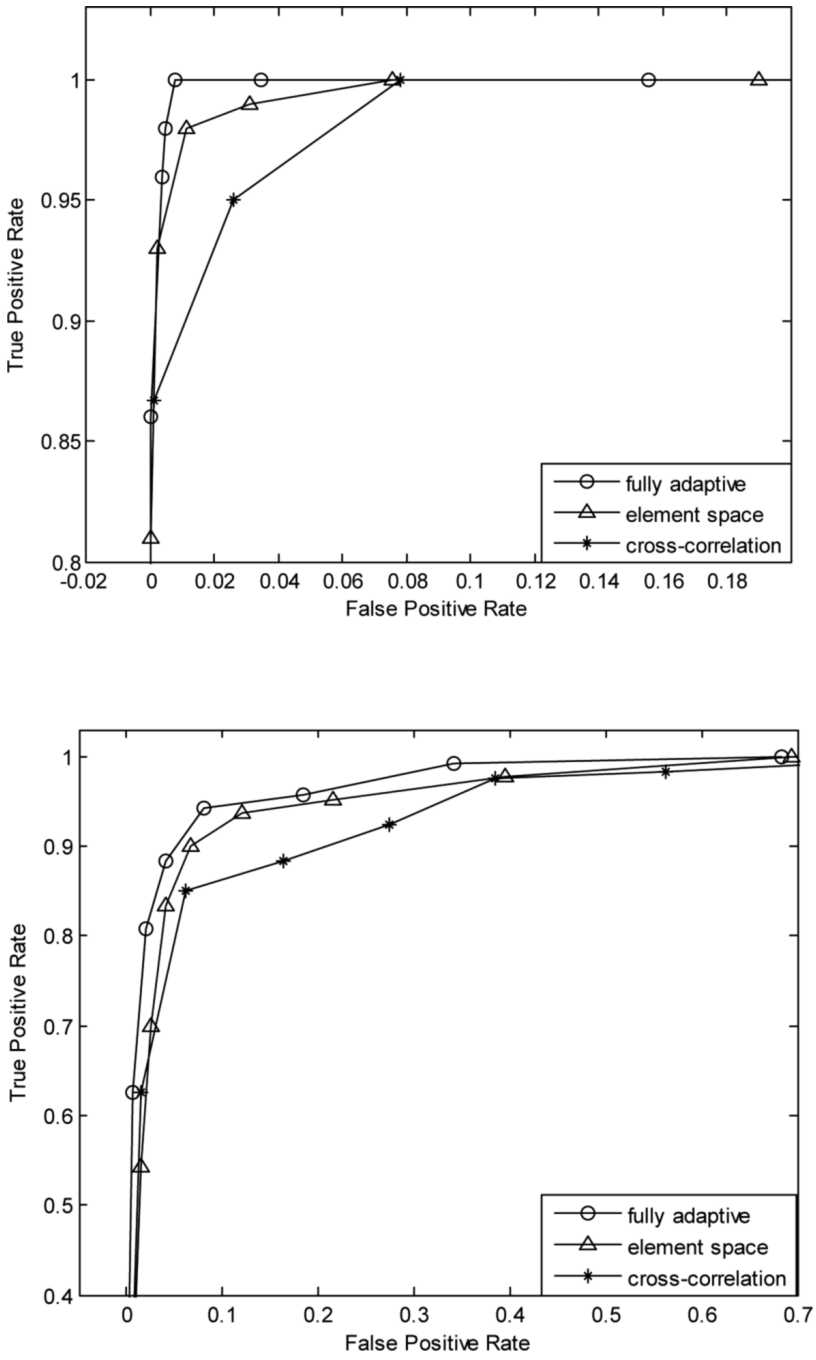

Fig. 2.

Comparison of receiver-operator characteristic (ROC) analysis of STAP algorithms and cross-correlation at response amplitudes of 4% (top three curves) and 2% (bottom three curves), relative to mean.

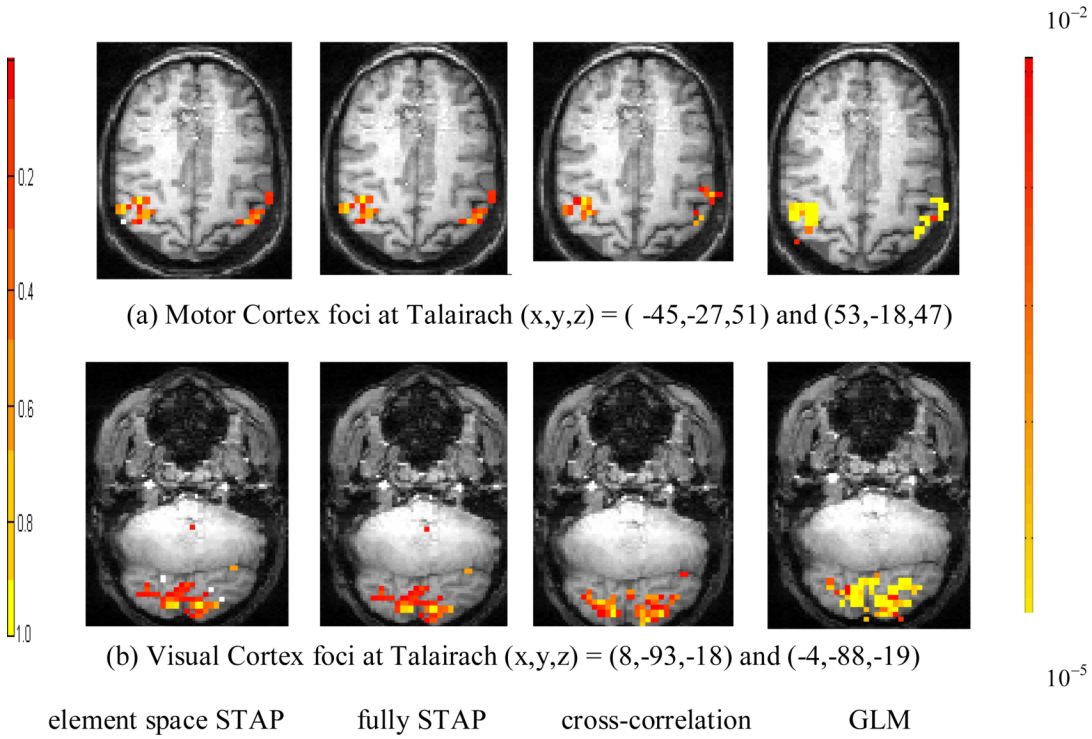

Fig. 3.

Activation maps for concurrent, but asynchronous finger-tapping (60s period) and visual stimulation (40s period) tasks for a single subject. Partially and fully adaptive STAP activation maps (threshold = 0.25, representing a fraction of the filter output having a range of 0-255; left colorbar) are contrasted with maps obtained using cross-correlation and the general linear model approach (thresholded such that $p \leq 0.01$, uncorrected for multiple comparisons; right colorbar). (a) Activation associated with the finger-tapping task, depicted at the level of the motor and somatosensory cortices. The peaks of the two depicted activations are at Talairach (x,y,z) = (-45, -27, 51) and (53, -18, 47). (b) Activation associated with the visual stimulation task, depicted at the level of the primary visual cortex. Left and right activation foci are at Talairach (x,y,z) = (-4, -88, -19) and (8, -93, -18).

TABLE I

Average True/False Positive performance for element space partially adaptive STAP as function of K_t

K_t (K_s=100)	Threshold								
	.1	.2	.3	.4	.5	.6	.7	.8	.9
1	10/52	10/13.3	10/2.3	**10/0**	**10/0**	**10/0**	8.8/0	6.3/0	3.8/0
2	10/53	10/13.3	10/2.3	**10/0**	**10/0**	**10/0**	8.5/0	6.3/0	3.8/0
3	10/51	10/13	10/2.3	**10/0**	**10/0**	**10/0**	8.8/0	6.3/0	3.8/0
4	10/51	10/13	10/2.3	**10/0**	**10/0**	**10/0**	8.8/0	6.3/0	3.8/0
5	10/52	10/13.3	10/2.3	10/0.3	**10/0**	**10/0**	8.5/0	6.3/0	3.5/0
6	10/50	10/12.8	10/2.3	**10/0**	**10/0**	**10/0**	9/0	6.3/0	3.8/0
10	10/45	10/13	10/2.3	**10/0**	**10/0**	**10/0**	9/0	6.8/0	3.8/0
12	10/40	10/15.2	10/2.3	10/0.3	9.8/0	9.8/0	9.2/0	6.9/0	4.2/0
15	10/41	10/15.2	10/2.3	10/0.3	9.8/0	9.8/0	9.2/0	6.9/0	4.2/0
20	10/41	10/15.5	10/2.2	10/0.3	9.8/0	9.8/0	9.2/0	6.9/0	4.2/0
30	10/45.3	10/20.8	10/3	**10/0.5**	**10/0**	**10/0**	9.3/0	6.8/0	3.8/0
60	10/51	10/13	**10/0**	**10/0**	**10/0**	**10/0**	9.3/0	6.9/0	4.2/0

IEEE Trans Biomed Eng. Author manuscript; available in PMC 2010 July 16.